Sensors and Materials, Vol. 38, No. 7 (2026) 4195–4206
MYU Tokyo

S & M 4558

Sensor-oriented Finite Element Analysis of Helmet Impact Response for Human Head Protection

Wei-Min Chi,[1,2] Rui-Ting Wei,[3] Chao-Ming Hsu,[3*] and Cheng-Fu Yang[4,5**]

[1]Elite Engineers College, Dongguan University of Technology, Dongguan5 23808, China
[2]Lunghwa University of Science and Technology, Department of Electronic Engineering, Taoyuan City 333, Taiwan
[3]Department of Mechanical Engineering, National Kaohsiung University of Science and Technology, Kaohsiung 807, Taiwan
[4]Department of Chemical and Materials Engineering, National University of Kaohsiung, Kaohsiung 811, Taiwan
[5]Department of Aeronautical Engineering, Chaoyang University of Technology, Taichung 413, Taiwan

(Received May 11, 2026; accepted July 3, 2026)

Keywords: helmet impact, finite element analysis, expanded polystyrene (EPS), acceleration response, stress distribution, impact biomechanics

Motorcycle transportation is widely used in densely populated regions, leading to frequent traffic accidents in which head injuries remain the leading cause of fatality. Helmets are therefore essential protective gear designed to reduce impact-induced damage to the human head. Beyond their traditional role, helmets can be regarded as sensor-interacting structures that not only absorb impact energy but also transform external mechanical stimuli into measurable physical responses. During an impact event, stress waves and deformation propagate through the helmet and are transmitted to the head, producing acceleration signals closely associated with injury severity. In this sense, acceleration serves as a key sensing output linking structural response to biomechanical evaluation. Finite element analysis is employed to investigate the dynamic behavior of a helmeted human head under various impact conditions. A three-dimensional model incorporating nonlinear expanded polystyrene behavior is developed to represent energy absorption characteristics. Multiple impact orientations are considered to evaluate stress distribution, displacement, and time-dependent responses. The results show that impact direction affects stress concentration patterns, whereas impact velocity governs the magnitude and evolution of the response. This sensing-oriented approach helps clarify the relationship between mechanical behavior and measurable signals, providing insights for helmet design optimization and advanced protective equipment.

1. Introduction

Motorcycle transportation remains one of the most widely adopted commuting methods in densely populated regions, particularly in Taiwan, where the number of registered motorcycles accounts for a substantial proportion of total vehicles. Although motorcycles offer advantages in

*Corresponding author: e-mail: jammy@nkust.edu.tw
**Corresponding author: e-mail: cfyang@nuk.edu.tw
https://doi.org/10.18494/SAM6416

ISSN 0914-4935
https://myukk.org/

flexibility, affordability, and accessibility, they are also associated with a high incidence of traffic accidents. Statistical data consistently indicate that head injuries are the leading cause of fatality in motorcycle-related crashes, often resulting in irreversible neurological damage or death within a short time after impact.(1,2) This critical safety concern highlights the indispensable role of helmets in mitigating head trauma. Consequently, helmets are not only regulatory safety equipment but also engineered protective systems designed to reduce the severity of impact forces.(3) A comprehensive understanding of how helmet structures interact with the human head under dynamic impact conditions is therefore essential for improving injury prevention strategies and advancing protective design.(4,5)

From an engineering and sensing perspective, modern helmets can be interpreted as sensor-interacting protective structures that actively mediate the transmission of mechanical signals. During an impact event, external kinetic energy is transferred into the helmet system and subsequently transformed into measurable physical quantities, including stress waves, deformation fields, and acceleration responses. Among these variables, acceleration is particularly significant because it can be directly measured using embedded or external sensors and is strongly correlated with injury severity. In this sense, the helmet functions not only as a passive energy absorber but also as a signal-conditioning medium that filters, redistributes, and attenuates mechanical inputs before they reach the skull and brain. This sensor-oriented interpretation provides a more integrated framework for evaluating helmet performance, linking structural mechanics with measurable biomechanical responses.

Finite element analysis (FEA) has become an indispensable tool for investigating impact biomechanics due to its capability to simulate complex interactions within heterogeneous materials and anatomical structures.(6,7) Compared with conventional experimental approaches, FEA offers high spatial and temporal resolution, enabling detailed visualization of stress propagation, deformation evolution, and acceleration time histories throughout the helmet–head system. In numerous studies, finite element models have been employed to examine helmet performance under different impact scenarios, focusing on factors such as shell material, liner properties, and geometric configurations. However, many existing works primarily emphasize structural response metrics without explicitly connecting these responses to sensing-related outputs. In particular, the interpretation of acceleration as a measurable signal that bridges simulation and real-world sensing data remains insufficiently explored.

The energy-absorbing liner, typically composed of expanded polystyrene (EPS), plays a critical role in determining the protective performance of helmets.(8) EPS exhibits highly nonlinear compressive behavior characterized by an initial elastic region, followed by a plateau region associated with cell collapse, and finally densification at high strains. This nonlinear response enables effective energy dissipation and reduction in peak acceleration transmitted to the head. Accurately modeling this behavior using a crushable foam material model is essential for capturing realistic impact dynamics. In addition, the direction and magnitude of impact significantly affect the distribution of stress, deformation, and acceleration within the protective system. Different impact orientations—such as frontal, lateral, rear, and top impacts—introduce distinct load paths and vibration modes, resulting in varying signal transmission characteristics. A multi-scenario analysis is therefore necessary to comprehensively evaluate the sensing and protective behavior of helmet systems.

In this study, a detailed finite element model of a helmeted human head is developed to investigate impact-induced dynamic responses under various loading conditions. The model incorporates anatomically representative head structures and a crushable foam material model for the EPS liner to accurately simulate its nonlinear energy absorption behavior. Multiple impact directions and velocities, consistent with standard testing conditions, are considered to analyze stress distribution, displacement evolution, and acceleration responses. By explicitly interpreting acceleration as a measurable sensing signal, we establish in this study a sensor-oriented analytical framework that connects mechanical response with potential injury mechanisms. The results not only provide insights into the effectiveness of helmet protection but also contribute to the development of advanced helmet systems that integrate sensing concepts with structural optimization, thereby supporting future smart protective technologies.

The sensing framework proposed in this study may also support the future integration of embedded sensing technologies within the helmet structure. For example, miniature accelerometers, pressure sensors, piezoresistive sensors, or flexible strain sensors can be embedded within the EPS liner to directly monitor impact-induced mechanical responses. Because the EPS liner is the primary energy-absorbing component of the helmet, sensors located within this region can provide valuable information regarding local deformation, stress transmission, and acceleration propagation during impact events. The combination of FEA and embedded sensing technologies can enable real-time impact monitoring, injury-risk assessment, and data-driven optimization of helmet designs, thereby contributing to the development of next-generation smart protective systems.

2. Experimental Procedure

The structural configuration of the helmet–head system is first established to define the sensing pathway through which impact-induced mechanical signals are transmitted. The helmet is composed of three primary layers: an outer shell, an energy-absorbing liner made of EPS, and an inner comfort padding layer, as illustrated in Fig. 1. The outer shell provides structural integrity and distributes localized impact forces, whereas the EPS liner plays a critical role in energy dissipation through nonlinear deformation. The inner padding ensures proper contact and fit between the helmet and the head. The human head model includes the skull and

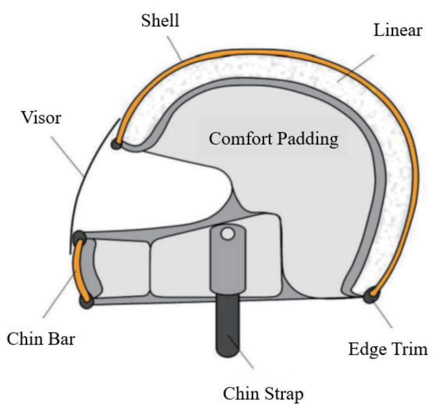

Fig. 1. (Color online) Schematic of helmet structure.

simplified brain structure, which together form a coupled biomechanical system. During impact, mechanical energy is transferred from the external surface of the helmet through the liner and subsequently into the skull and brain tissues. In this study, this transmission process is interpreted as a sensing pathway, where stress waves and acceleration signals propagate across different material interfaces. Acceleration, in particular, is treated as a representative measurable signal that reflects the effectiveness of impact mitigation and serves as a bridge between simulation outputs and real-world sensor measurements.

A three-dimensional finite element model of the helmet–head system is constructed to simulate dynamic impact behavior. The integrated model, shown in Figs. 2(a) and 2(b), consists of the helmet assembly and the human head positioned in close contact. The geometric models are imported into the finite element environment and aligned to ensure proper interaction between components. Material properties are assigned on the basis of the literature and engineering approximations. The helmet shell is modeled as a linear elastic material, whereas the EPS liner is defined using a crushable foam model to capture its nonlinear compressive behavior under impact loading. The material parameters of the EPS liner were adopted from previously published experimental studies on crushable foam behavior and helmet impact analysis. These parameters have been widely used to represent the nonlinear compression and energy-absorption characteristics of EPS under dynamic loading conditions. The present study focuses on the comparative effects of impact direction and velocity; therefore, literature-based parameters were employed rather than conducting a dedicated material calibration procedure. Although the adopted parameters provide physically reasonable impact responses, future work will incorporate experimental compression testing of EPS specimens and instrumented helmet impact experiments to calibrate the material model and quantitatively validate the predicted acceleration responses. The skull is modeled as an elastic structure with higher stiffness, whereas the brain tissue is assigned relatively softer material properties to represent its deformable nature. Contact interactions between the helmet and the head are defined to allow force transmission while preventing unrealistic penetration. To ensure numerical accuracy, appropriate boundary conditions and initial conditions are applied. The base of the model is constrained to simulate a fixed reference frame, and initial velocities are assigned to represent impact conditions consistent with standard helmet testing scenarios.

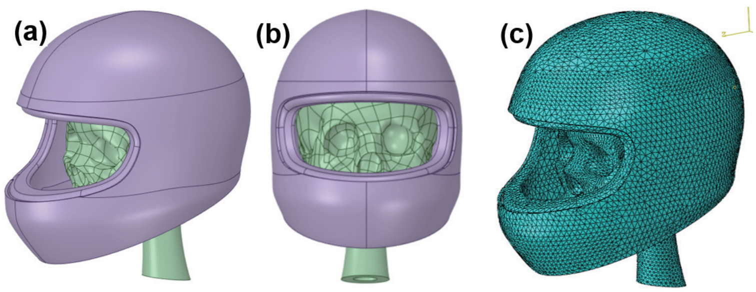

Fig. 2. (Color online) Meshed model of the helmet–head system.

These configurations enable the simulation of realistic impact events while maintaining computational stability. The finite element mesh is generated to balance computational efficiency and solution accuracy. The meshed model is shown in Fig. 2(c), where finer mesh regions are applied to areas expected to experience high stress gradients, such as the contact interfaces between the helmet liner and the skull. Coarser mesh regions are used in less critical areas to reduce computational cost. Higher-order solid elements are employed to improve solution accuracy, particularly in capturing complex deformation and stress wave propagation during impact. Mesh quality is carefully evaluated to avoid numerical issues such as element distortion and instability. Although detailed mesh convergence plots are not explicitly presented here, convergence analysis is conducted during model development to ensure that further mesh refinement does not significantly alter key output parameters, such as peak stress and acceleration. The mesh configuration also plays a crucial role in accurately capturing acceleration signals, which are sensitive to local deformation behavior. Therefore, particular attention is given to regions where acceleration data are extracted, ensuring that the mesh resolution is sufficient to reflect realistic dynamic responses.

Dynamic impact simulations are performed using explicit time integration to capture high-speed transient responses. Multiple impact scenarios are defined on the basis of standard testing conditions, including variations in impact direction (front, rear, top, and lateral) and impact velocity. These scenarios are designed to represent realistic accident conditions and to investigate the influence of impact orientation on signal transmission within the helmet–head system. During each simulation, key physical quantities—including stress, displacement, and acceleration—are recorded at predefined locations. Acceleration data are extracted from the head model to represent the measurable sensing signal associated with injury assessment. The temporal evolution of these signals provides insight into how the helmet structure modifies the incoming impact energy. In addition, the nonlinear deformation of the EPS liner is monitored to evaluate its energy absorption capability. The compression behavior of the foam directly influences the magnitude and duration of acceleration peaks, thereby affecting the overall protective performance of the helmet. The simulation framework enables a comprehensive evaluation of both structural behavior and sensing characteristics by analyzing these dynamic responses.

The simulation outputs are processed to obtain time-dependent response curves for stress, displacement, and acceleration. These results are analyzed to identify peak values, response durations, and spatial distributions within the helmet–head system. Acceleration signals are of particular interest, as they are directly related to injury metrics and can be compared with sensor-based measurements in practical applications. To enhance interpretability, the results are compared across different impact conditions, allowing for the identification of critical scenarios that produce the highest mechanical loads. The relationship between structural response and measurable signals is further examined to establish a sensing-oriented understanding of helmet performance. This approach provides not only a mechanical evaluation but also a framework for integrating simulation results with real-world sensing systems, thereby supporting the development of advanced protective technologies.

3. Results and Discussion

The impact responses of the helmet–head system are evaluated in terms of stress distribution under four representative impact orientations, including frontal, rear, top, and lateral impacts. As shown in Fig. 3(a), the frontal impact produces a localized stress concentration at the contact region between the helmet shell and the rigid surface. The stress is initially borne by the shell and then transmitted into the EPS liner, where it is attenuated through compressive deformation. This indicates that the helmet redistributes incoming impact energy and modifies the resulting mechanical response. A similar concentration at the contact interface is observed in the rear impact [Fig. 3(b)], although the stress distribution appears slightly broader owing to differences in geometry and structural support. For the top impact [Fig. 3(c)], the stress distribution is more symmetric and spreads over a larger area, leading to reduced stress concentration and more uniform EPS deformation. In contrast, the lateral impact [Fig. 3(d)] exhibits a more complex and asymmetric distribution, with localized stress concentration and uneven deformation caused by geometric curvature and lower structural stiffness. Stress is consistently concentrated at the helmet shell–rigid surface contact region, whereas its propagation and attenuation are influenced by impact direction and structural characteristics. The nonlinear behavior of the EPS liner plays a key role in reducing stress intensity and modifying the transmitted mechanical response, which is directly related to measurable signals such as acceleration.

The frontal impact data point is defined at the red marker in Fig. 3(a), enabling the extraction of time-dependent responses. Figure 3(a) shows that the highest stress is concentrated at the contact interface between the helmet shell and the rigid surface. This confirms that the initial load transfer is dominated by direct contact mechanics, with stress rapidly propagating from the shell into the underlying EPS liner. Figure 4(a) illustrates the time histories of equivalent stress at the frontal impact point under different impact velocities. The results show that the initial contact between the helmet and the rigid surface occurs at approximately 0.5 ms, at which point a sharp rise in stress is observed. The peak stress values corresponding to increasing impact velocities are 91.3, 149.2, and 177.4 MPa, indicating a clear velocity-dependent amplification of mechanical loading. The predicted acceleration trends are consistent with the general behavior reported in the literature on helmet impact, where increasing impact velocity leads to higher peak head acceleration and greater injury risk. For the 4 and 6 m/s impacts, a secondary stress peak is observed at approximately 4 ms, which can be attributed to rebound-induced re-contact

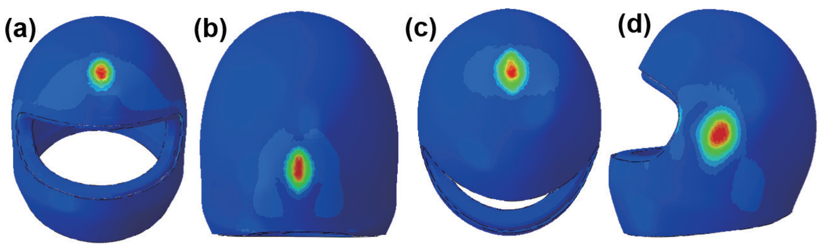

Fig. 3. (Color online) (a) Stress distribution and equivalent stress distribution at different impact points of the helmet: (a) frontal, (b) rear, (c) top, and (d) lateral.

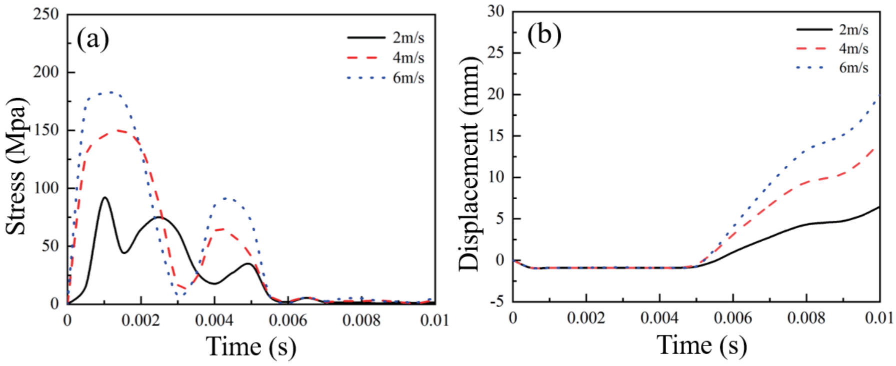

Fig. 4. (Color online) Stress and displacement responses at the frontal impact point of the helmet under different velocities: (a) equivalent stress versus time and (b) *Z*-axis displacement versus time.

between the deformed helmet shell and the rigid surface. In the 2 m/s impact, an additional peak appears earlier, at approximately 2.5–3 ms. This earlier peak is also associated with the contact–separation–recontact process, but occurs sooner because the lower impact energy results in reduced deformation of the helmet structure and EPS liner, leading to an earlier rebound response. These observations indicate that the timing of secondary peaks depends on not only the occurrence of rebound but also the impact velocity and the resulting deformation characteristics of the helmet system. This phenomenon reflects the dynamic interaction between structural deformation and contact conditions, and suggests that impact events may involve multiple loading cycles rather than a single impulse. From a sensing perspective, such secondary peaks may contribute to complex acceleration signatures, potentially affecting injury assessment.

Figure 4(b) shows the *Z*-axis displacement–time response at the same location. A negative displacement is observed prior to 0.5 ms, representing the approach phase before contact with the rigid surface. After impact, the displacement remains relatively stable for a short duration owing to energy absorption by the EPS liner. Beyond approximately 5 ms, the displacement begins to increase, indicating that the helmet rebounds and gradually separates from the rigid surface. At 10 ms, the displacements for the 2, 4, and 6 m/s impacts are 6.45, 14.23, and 20 mm, respectively. These results demonstrate that higher impact velocities lead to greater deformation and rebound displacement. The increased displacement is associated with higher stored elastic and recoverable energy within the helmet structure, which also correlates with more pronounced dynamic responses. Overall, the combined stress and displacement results reveal that impact velocity plays a critical role in governing both the magnitude and temporal characteristics of the mechanical response. The presence of secondary impacts and velocity-dependent deformation further highlights the importance of considering dynamic interactions when evaluating helmet performance. These findings provide valuable insights into how impact energy is transformed within the helmet system and how such transformations influence measurable signals, particularly acceleration, which is directly related to injury risk.

The rear impact data point is defined at the red marker in Fig. 3(b) at the contact region. Figure 3(b) shows the corresponding equivalent stress distribution. Figure 5(a) shows the equivalent stress–time histories at the rear impact point under different impact velocities. The

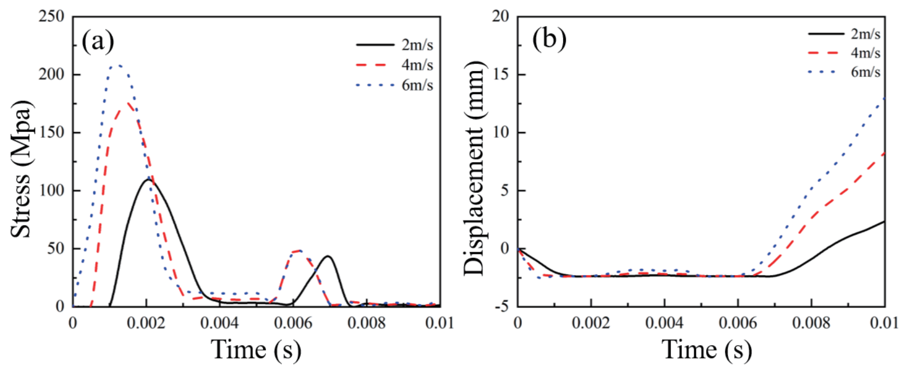

Fig. 5. (Color online) Stress and displacement responses at the rear impact point of the helmet under different velocities: (a) equivalent stress versus time and (b) *Z*-axis displacement versus time.

results indicate that contact between the helmet and the rigid surface occurs at approximately 1 ms, as evidenced by the rapid rise in stress. The peak stress values for the 2, 4, and 6 m/s impacts are 112.1, 175.4, and 203.8 MPa, respectively, demonstrating a clear velocity-dependent increase in mechanical loading. A secondary peak is observed at around 6.2 ms, which can be attributed to rebound-induced re-contact between the deformed helmet shell and the rigid surface. This phenomenon indicates that the impact process involves multiple interaction stages rather than a single event. Although the overall trends of the curves are similar, the 2 m/s impact shows a delayed contact time compared with higher velocities, reflecting the influence of initial velocity on impact timing and energy transfer.

From a mechanical and sensing perspective, the presence of secondary peaks suggests more complex acceleration-related sensing signal patterns, including multiple response peaks and variations in signal timing. These characteristics may influence the interpretation of impact severity and injury assessment. Figure 5(b) shows the *Z*-axis displacement–time responses at the same location. A negative displacement is observed before 1 ms, representing the pre-impact motion toward the rigid surface. After contact, the displacement changes only slightly owing to the energy absorption by the EPS liner. Beyond approximately 6 ms, the displacement gradually increases, indicating that the helmet rebounds and separates from the rigid surface. At 10 ms, the displacements for the 2, 4, and 6 m/s impacts are 2.3, 8.3, and 13 mm, respectively. These results show that higher impact velocities lead to greater deformation and rebound displacement, which are associated with increased stored and released elastic energy. This behavior also implies that higher velocities may generate stronger and more prolonged dynamic responses, further influencing the characteristics of measurable signals such as acceleration.

The data acquisition point for the top impact is defined at the red marker shown in Fig. 3(c), located at the contact region to capture the time-dependent response during impact. Figure 3(c) shows the equivalent stress distribution at the top impact point. Figure 6(a) shows the equivalent stress–time histories at the top impact point under different impact velocities. The results indicate that contact between the helmet and the rigid surface occurs at approximately 1 ms, as evidenced by the rapid increase in stress. The peak stress values for the 2, 4, and 6 m/s impacts are 152.6, 229.3, and 263.2 MPa, respectively, demonstrating a clear velocity-dependent increase

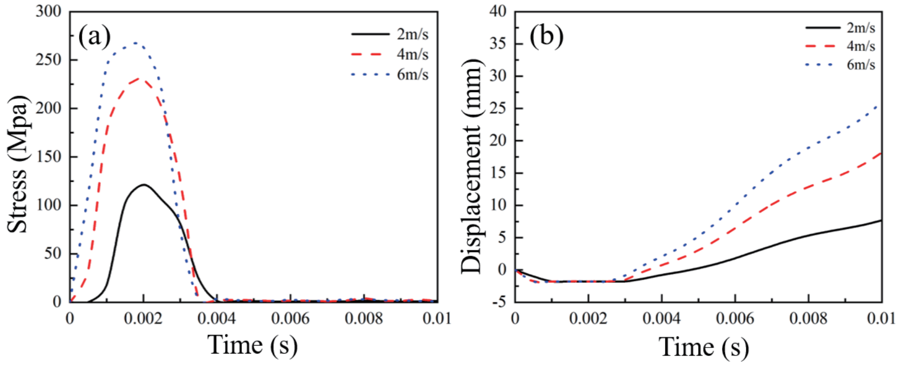

Fig. 6. (Color online) Stress and displacement responses at the top impact point of the helmet under different velocities: (a) equivalent stress versus time and (b) *Z*-axis displacement versus time.

in mechanical loading. Unlike the frontal and rear impacts, no secondary peak is observed in the stress–time curves. This suggests that the top impact leads to a more stable contact condition with reduced rebound-induced re-contact. The smoother stress evolution indicates that the load is more uniformly distributed and absorbed, which can reduce abrupt fluctuations in the transmitted mechanical signals. From a sensing perspective, this implies a cleaner and more predictable signal profile, which is advantageous for interpreting acceleration-based injury metrics.

Figure 6(b) shows the *Z*-axis displacement–time responses at the same location. A negative displacement is observed prior to 1 ms, representing the approach of the helmet toward the rigid surface. After impact, the displacement remains relatively stable for a short duration owing to energy absorption by the EPS liner. Beyond approximately 3 ms, the displacement gradually increases, indicating that the helmet rebounds and moves away from the rigid surface. At 10 ms, the displacements reach 7.6, 18.1, and 26 mm as the impact velocity increases from 2 to 6 m/s. These results confirm that higher impact velocities result in greater deformation and rebound displacement. The absence of significant oscillations in displacement further supports the observation of reduced secondary interactions. This behavior suggests that top impacts may produce more stable dynamic responses, with lower variability in mechanical signals, thereby improving the reliability of sensing-based evaluations.

The data acquisition point for the lateral impact is defined at the red marker shown in Fig. 3(d), positioned at the contact region to capture the time-dependent response during impact. Figure 3(d) shows the equivalent stress distribution at the lateral impact point. Figure 7(a) shows the equivalent stress–time histories at the lateral impact point under different impact velocities. The results indicate that contact occurs at approximately 0.5 ms, as evidenced by the initial rise in stress. The peak stress values increase from 56.3 to 77.6 MPa as the impact velocity increases, indicating a velocity-dependent increase in mechanical loading, which are noticeably lower than those observed in the frontal, rear, and top impacts. This difference can be attributed to the larger and relatively flatter contact area during lateral impact, which allows the load to be distributed more evenly and reduces localized stress concentration. However, it is observed that the maximum stress shifts to the visor detachment region, indicating a potential structural

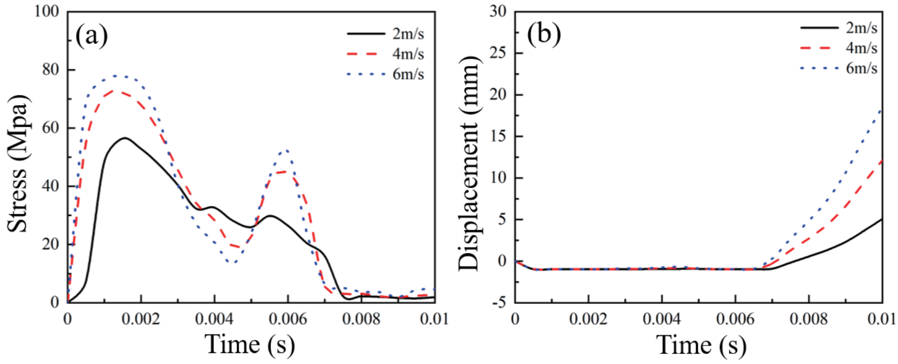

Fig. 7. (Color online) Stress and displacement responses at the lateral impact point of the helmet under different velocities: (a) equivalent stress versus time and (b) Z-axis displacement versus time.

weakness where failure may occur. This finding highlights that even when overall stress levels are lower, localized stress concentration at geometrically discontinuous regions can still pose a risk of damage. As expected, higher impact velocities lead to increased stress levels, although the rate of increase is not strictly proportional.

Figure 7(b) shows the Z-axis displacement–time responses for the lateral impact. A displacement variation is observed prior to 0.5 ms, representing the approach phase before contact. After impact, the displacement remains relatively stable for a short duration owing to energy absorption within the helmet structure. At approximately 6.5 ms, the helmet begins to rebound and gradually moves away from the rigid surface. At 10 ms, the displacements are 5, 12.1, and 18.5 mm for impact velocities of 2, 4, and 6 m/s, respectively. These results indicate that higher impact velocities result in greater deformation and rebound displacement. The rebound behavior reflects the release of stored elastic energy and contributes to the dynamic response characteristics of the helmet system. Overall, the results indicate that the top impact produces the highest stress and displacement, whereas the lateral impact yields lower overall stress owing to a larger contact area. However, the lateral impact reveals critical localized stress at the visor mounting region, suggesting a potential failure location. In addition, the peak stress values do not increase linearly with impact velocity, indicating the influence of nonlinear material behavior and structural interaction. The displacement responses further show that rebound is a consistent phenomenon across all cases, with higher velocities leading to greater rebound distances. These findings emphasize the importance of considering both global response and local structural vulnerability in helmet design and performance evaluation.

From a biomechanical perspective, acceleration responses obtained from the helmet–head system may also be used to derive injury assessment metrics such as the head injury criterion (HIC). Since HIC is widely adopted in helmet certification and impact-safety evaluation, it provides a quantitative measure linking acceleration exposure to potential injury severity. Although the present study focuses on relative comparisons of mechanical responses under different impact conditions, the predicted acceleration signals establish a foundation for future injury-risk assessment. Future work will incorporate detailed acceleration–time histories and experimentally validated models to calculate HIC and other biomechanical injury metrics, thereby strengthening the connection between sensing outputs and injury evaluation.

Note that the present helmet–head model adopts a simplified representation of the human head and therefore does not explicitly include cerebrospinal fluid, intracranial pressure effects, detailed brain–skull coupling, or brain tissue shear strain responses. Consequently, the current analysis focuses primarily on the transmission of mechanical loads, stress distributions, deformation behavior, and acceleration-related sensing signals rather than detailed neurological injury mechanisms. Although the simplified model is sufficient for investigating the relative influence of impact direction and velocity on helmet performance, it may not fully capture the complex biomechanical responses occurring within the cranial cavity. Future studies will incorporate anatomically detailed head models with fluid–structure interaction capabilities, allowing the evaluation of intracranial pressure distributions, brain tissue deformation, and shear strain responses. Such improvements will enable a more comprehensive assessment of both protective performance and injury risk while further strengthening the proposed sensor-oriented framework. Furthermore, embedded acceleration and pressure sensors may be integrated with the enhanced model to establish correlations between measurable sensing signals and intracranial biomechanical responses, thereby supporting the development of next-generation smart helmet systems for real-time injury assessment.

Although the present finite element model provides detailed insights into stress propagation, deformation behavior, and acceleration-related sensing responses, the results are currently based on numerical simulations without direct experimental validation. The material parameters, contact definitions, and impact conditions adopted in this study were selected according to published literature and standard helmet testing scenarios to ensure realistic modeling conditions. Therefore, the current results are primarily intended to determine the relative influence of impact direction and velocity on the dynamic response of the helmet–head system. Future work will include instrumented impact experiments using accelerometers and standardized headform tests to quantitatively validate the predicted stress, displacement, and acceleration responses and further improve the reliability of the proposed sensor-oriented framework.

4. Conclusions

A sensor-oriented FEA of helmet impact response is conducted to examine the transformation and redistribution of mechanical signals within the helmet–head system under multiple impact conditions. The results show that stress is consistently concentrated at the contact interface between the helmet shell and the rigid surface, whereas its magnitude and distribution vary with impact orientation. Among the examined cases, the top impact produces the highest stress and displacement owing to more direct load transmission, whereas the lateral impact yields lower overall stress because of a larger contact area, despite revealing localized stress concentration at the visor mounting region, indicating a potential structural weakness. Temporal responses further indicate that impact velocity plays a critical role in governing both peak stress and dynamic behavior. Higher velocities result in increased stress levels and larger deformation, although the increase is not strictly proportional owing to nonlinear material effects and structural interactions. In several cases, secondary stress peaks are observed, reflecting rebound-induced re-contact and suggesting that the impact process involves multiple loading stages. Displacement results consistently show rebound behavior after impact, with greater rebound distances observed at higher velocities, corresponding to increased stored and released energy within the helmet structure. From a sensing perspective, these findings illustrate how mechanical energy is transformed into measurable signals through stress evolution and deformation, which directly influence acceleration responses. The variations across different impact directions highlight the importance of considering both global structural behavior and local stress concentration in performance evaluation. Overall, a unified framework linking structural response with sensing outputs is established, providing practical insights for helmet design optimization. These results also support the development of advanced protective systems with improved reliability and potential integration of sensing technologies for real-time impact monitoring and injury assessment.

Acknowledgments

This work was supported by the Guangdong Provincial Department of Science and Technology under Grant No. 2024A0505050048. This work was also supported by Summit-Tech Resource Corp., and by projects under Nos. NSTC 113-2221-E-390-011 and NSTC 114-2622-E-390-001.

References

1 M. Banson, M. K Ametefe, K. Darko, J. C. B. Dakubo, M. Iddrisu, and T. Dakurah: J. West. Afr. Coll. Surg. **15** (2024) 75.
2 H. G. Al-Anbari and N. M. S. Al-Zaubai: Int. J. Front. Med. Surg. Res. **07** (2025) 001.
3 https://www.hseblog.com/understanding-safety-helmet-standards/ (accessed July 2023).
4 M. Nasim, S. Spadoni, P. G. Pavan, V. Brasco, and U. Galvanett: J. Biomech. **176** (2024) 112362.
5 V. Varanges, P. Eghbali, N. Nasrollahzadeh, J. Y. Fournier, P. E. Bourban, and D. P. Pioletti: Commun. Eng. **4** (2025) 22.
6 C. Stephen, B. Shivamurthy, R. Selvam, S. R. Behara, A. H. I. Mourad, and S. Kannan: Mater. Today: Proc. **56** (2022) 3636.
7 T. V. Minh and T. T. Tran: Eng. Res. Express **7** (2025) 045430.
8 M. Arnesen, S. Hallstrom, P. Halldin, and A. Kulachenko: Results Eng. **23** (2024) 102685.